

RESEARCH

Open Access



Non-invasive analysis of heritage textiles with MA-XRF mapping—exploring the possibilities. The study of Bishop Jacques de Vitry's mitres and fragile medieval reliquary purses from Namur (Belgium)

Ina Vanden Berghe^{1*}, Marina Van Bos¹, Maaïke Vandorpe¹ and Alexia Coudray¹

Abstract

This manuscript explores the potential of macro-X-ray fluorescence (MA-XRF) for the non-invasive analysis of heritage textiles. XRF, especially with the portable instruments, is a well-known technique for the non-destructive examination of various cultural heritage objects. It allows analysis of elemental composition based on single-point measurements. However, large, or complex textiles require numerous analysis points to identify the materials used and correctly interpret the spectra. MA-XRF takes this type of research to the next level, as it is possible to visualise the element distribution over an entire mapped area. In this paper, we discuss the application of this technique to the study of complex and multi-layered textile objects from exceptional Belgian heritage collections, including two mitres attributed to Bishop Jacques de Vitry, dating between twelfth and thirteenth century, and two of the seven extremely fine medieval reliquary purses from Namur. These are very fragile, richly decorated textile objects whose current state of preservation is a major impediment to sampling. MA-XRF mapping was applied for the identification of the elements of different materials in a non-invasive manner, including metal threads, ink, dyes, and various materials used in illuminations. In addition to material identification, stratigraphic information was obtained from the visualisation of element distributions, and hidden structural details were discovered. MA-XRF was also tested on some areas with more relief, such as the embroidery and braid made with metal threads, and the undulated multi-layered structure of the parchment mitre. Even though the analyses here could not be carried out in optimal conditions, these locations could also be analysed, albeit at a lower resolution. Finally, the technique proved very effective as a tool for screening, allowing samples to be taken at a more informative and representative location and minimising sampling.

Keywords Macro-X-ray fluorescence, MA-XRF, Non-invasive, Textiles, Reliquary purses, Mitres, Jacques de Vitry, Belgian heritage, Metal threads, Embroidery, Illumination

Introduction

Heritage textiles are an important testimony to past societies. They not only provide information about material knowledge and skills; their study can provide clues to the influences, interactions, and trade practices between societies. However, the material investigation of textiles is often complex. Textile objects are discovered only sporadically, and since they consist mainly of organic

*Correspondence:

Ina Vanden Berghe
ina.vandenbergh@kikirpa.be

¹ Royal Institute for Cultural Heritage, Jubelpark 1, 1000 Brussels, Belgium

material, they are often found in a highly altered state, with the extent of degradation varying greatly due to different burial or preservation conditions and other external influences [1–6].

This results in specific challenges for the material identification of preserved textiles. Identification of the different components of the textile, including fibres, dyes or pigments, mordants and metal threads, and of the thread and weave structure as such, is complicated by the state of degradation of each material. Furthermore, the overall impaired to poor condition of the textile may complicate the manipulation of the object. Drastic conservation treatments may be necessary to save the textile from further decay, and such situations may complicate or prevent sampling.

Established techniques to elucidate the organic and/or inorganic constituents in textile artefacts include optical microscopy, liquid (LC) and gas (GC) chromatography, micro-Raman spectroscopy (MRS), attenuated total reflectance Fourier transform infrared spectroscopy (ATR-FTIR), scanning electron microscopy with energy-dispersive X-ray detection (SEM-EDS) and X-ray fluorescence spectroscopy (XRF) [1–3, 6–11]. These techniques are micro-destructive or non-invasive and are all performed on very small samples or very small areas of the textile.

XRF has been used for many years for the non-destructive analysis of various objects of cultural heritage [12–15]. It is an established technique for the study of inorganic elements due to its non-invasiveness, speed of analysis, and spatial resolution. However, there are also drawbacks. XRF measurements are often single point measurements with spot sizes that range from a few mm to less than 100 μm using poly capillary optics. However, numerous single-point analyses are required to identify the materials used, and the correct interpretation of so many individual spectra can be very time-consuming. Furthermore, inorganic materials present in different layers or in the matrix around the object of investigation all produce secondary X-rays, which complicates the interpretation of results, as signal from all layers are obtained in one measurement. In addition, only local point information is obtained, which may not be representative of the entire object. This is especially disadvantageous for textiles in highly degraded or fragile condition or for archaeological textiles, for which the visual selection of points for analysis can be very limited or difficult.

The addition of MA-XRF, developed for and used mainly in painting research over the last decade, resolves some of the previously described drawbacks [16–21]. With MA-XRF, the X-ray beam scans areas of interest or even the entire object, and thousands and sometimes millions of data points are produced. In this way, the data

are plotted as elemental distribution maps. These plots facilitate interpretation by revealing the localization and relative intensity of elements in a single map. Since the analysed points cover a large area, it is also easier to estimate to what extent they are representative or occur in the entire object. In addition, these images help to decipher original motifs that are no longer visible, underlying structures, or materials that are partially lost or difficult to trace visually. This technique has already proven useful for the material analysis of heritage objects including illuminated manuscripts, stained-glass windows, embroidered leather, paintings and dyes [22–27]. Although stratigraphic analyses are usually complex or sometimes not possible in cultural heritage objects, MA-XRF, in combination with other analytical techniques, can be used for the study of pigments in multi-layered structures by visual assessment of the suppression or transmission of signals from different elements [26–29]. Furthermore, the intuitive nature of element maps offers added value compared to data from point analyses in an interdisciplinary setting, enabling archaeologists, historians, conservators and others not specialized in X-ray techniques to participate more easily in discussions of results. Finally, MA-XRF mapping can be of particular interest to minimize sampling for further micro-destructive analyses.

This paper focuses on new possibilities offered by MA-XRF mapping for non-invasive, in-situ material identification in complex heritage textiles. The potential of this technique is explored and discussed through its application to two case studies of important Belgian heritage objects: two thirteenth century Episcopal mitres, ascribed to Bishop Jacques de Vitry and belonging to the Relic Treasure of Oignies, and two extremely fine and fragile medieval reliquary purses, part of an ensemble of seven purses preserved in the Provincial Museum of Ancient Art, Namur, Belgium.

Materials and methods

Heritage textiles under investigation

Episcopal mitres

The two Episcopal mitres with skeletal remains are part of the reliquary ascribed to Bishop Jacques de Vitry, who was born in Champagne in approximately 1165–1170 and died in Rome in 1240. After his death, the mitres were transferred along with the remains to the St. Nicolas Church in Oignies, Belgium. In 1818, the treasure was donated to the Congregation of the Sisters of the Notre-Dame, who ceded it to the King Baudouin Foundation in 2010. Since then, it has been exhibited at the Museum of Ancient Art in Namur (TreM.a) under the scientific responsibility of the Archaeological Society of Namur. The Relic Treasure of Oignies includes multiple objects

listed as exceptional moveable cultural heritage by the Brussels-Walloon Federation and was assigned as one of the Seven Wonders of Belgium [30–32].

The illuminated parchment mitre is unique because it is the only one known to feature parchment decorations, which are richly embellished with miniatures. It was made in a workshop in Paris and was likely only used for important ceremonies [30]. The embroidered mitre is made of textile with metal thread embroidery in *opus anglicanum*, likely manufactured in an English workshop [30, 33]. The two mitres are multi-layered structures composed of a complex combination of materials that exhibit diverse degradation phenomena.

The illuminated parchment mitre (Fig. 1b–d) has a primary structure of white leather covered with an ecru silk fabric, on which bands of parchment with polychrome decorations are applied. The silk fabric itself has painted decorations including a star and a moon and is currently in a very degraded state. Holes and tears are visible in many places. The mitre is fitted with two long fanons covered at the outer side with painted parchment decorations and lined with a red fabric at the back. At the front

of the fanons, the attachment of the red lining is visible, as well as remnants of a black galloon. The fanons originally had fringes, of which some remnants of green and brown threads are preserved. Furthermore, the back of the mitre contains a wide braided band in the middle, made with a combination of metal threads and ochre/green textile threads. This wide braid was probably an intermediate piece added to customise the head circumference of the mitre.

The textile mitre is completely different. It is made of textile and contains representations embroidered with metal threads (Fig. 1a–c). The front side of the mitre head has large gaps and depicts the martyrdom of St Laurentius. It shows two torturers holding forks and whips turning the body of Saint Lawrence on a grate above the flames. The inscription S[AN]C[TV]S LAVREN-CIVS confirms the martyr's identity. The back of the mitre depicts Thomas Becket falling before an altar, with his back to the three knights who took part in his murder on 29 December, one of whom is striking his head with a sword. An embroidered inscription mentions the name of Saint Thomas Becket (S[AN]C[TV]S THOMAS) [30]. The embroidered mitre is composed of a coarse textile fabric in linen as the primary structure. This textile is completely covered with a fine white silk samite in twill weave which is in very poor condition. This mitre has no painted decorations but is richly decorated by embroidery in metal thread. The two fanons have the same textile composition and are also decorated with metal thread embroidery. On the edges of the fanons, remnants of a red silk tabby fabric are visible, dyed with the precious red from kermes, which was attached under a galloon consisting of metal threads and black stripes. The red silk is not present at the back of the fanons. These are instead lined with a yellow silk lining, suggesting that the original red lining was replaced with the yellow during an earlier restoration. The fanons contain fringes of different colours [30].



Fig. 1 The mitre with metal thread embroidery, front and reverse side (a–c), and the illuminated parchment mitre, front and reverse side (b–d) (reduced image resolution; images©KIK-IRPA, Brussels)

Medieval reliquary purses

Seven reliquary pouches belong to the Provincial Museum of Ancient Arts of Namur (TreM.a) in Belgium. According to the visitor guide *Les peintures à l'aiguille*, five reliquary purses were preserved by the former keeper of the relics of the canon of Hautregard in Namur, while two came from Hastière [34]. Except for one purse made of leather, they are all made of silk and/or linen, and several are embroidered with silk and metal threads. The objects, dating between the eleventh and fifteenth century have been exhibited in the museum for many years and have become extremely fragile. Between 2019 and 2020, they were studied at



Fig. 2 Reliquary purse 229d (a), measuring 119 mm × 124 mm; reliquary purse 229f (b), measuring 165 mm × 165 mm (reduced image resolution; images©KIK-IRPA, Brussels)

the occasion of their conservation at the Royal Institute of Cultural Heritage (KIK-IRPA) in Brussels, Belgium. Two of these exceptional reliquary pieces are discussed in this paper.

The purse 229d is a small pouch made of silk woven in very fine tapestry technique (dimensions 119 mm × 124 mm). It has five bands on both sides alternating between green and pink on which four different coats of arms have been woven in metal threads. The repetitive decorative pattern refers to a Spanish origin from the thirteenth century onwards. The pouch was radiocarbon dated to a period between 1150 and 1250 AD (80% confidence interval). It is very small and fragile. The cords are broken in several places and have been tied back together. The purse has no lining, although there likely was one originally (Fig. 2a) [35].

The second purse 229f is a small, fringed purse (dimensions 165 mm × 165 mm) possibly from Hastière. It was radiocarbon dated to between 1260 and 1310 AD (77.4% confidence interval). This purse is made in needlework technique and is bordered with a decoration of Turk's head knots made of metal threads. Along the bottom there are alternating large and small knots, and the five large ones have fringes. On one side, the purse contains a *cedula*, a small parchment banner with a possible inscription. At the top, the two ends of the suspension cord

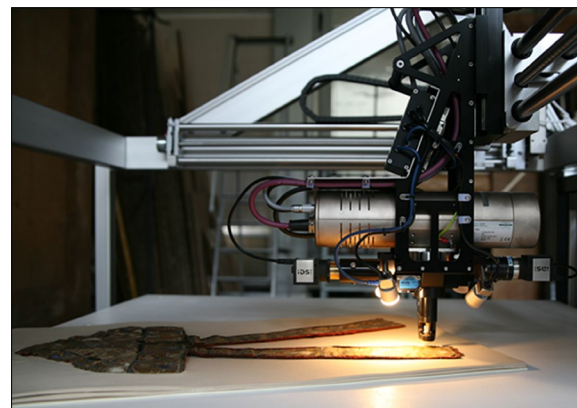


Fig. 3 MA-XRF mapping with the Bruker M6 Jetstream large area scanner (images©KIK-IRPA, Brussels)

have been attached. The purse is lined with a silk taffeta divided into two compartments. Several remains of bone were found inside (Fig. 2b) [35].

Method

The MA-XRF mapping measurements were performed using the M6 Jetstream large-area scanner (Bruker Nano Analytics) with a rhodium-target microfocus X-ray tube, operating at 600 μ A current and 50 kV, and a 30 mm²



Fig. 4 The undulated mitre surface (images©KIK-IRPA, Brussels)

X-Flash silicon drift detector (Fig. 3). The measuring head is mounted on an XY-motorized stage with maximum travelling range of 80×60 cm in steps as small as $10 \mu\text{m}$. The beam spot size is adjustable between 50 and $500 \mu\text{m}$ based on the selection of one of five predefined steps (50 , 150 , 250 , 400 or $500 \mu\text{m}$). The instrument is operated in open atmosphere and provides qualitative data for elements whose atomic number is equal to or greater than that of aluminium ($Z = 13$). The XRF spectra of the mitres were collected, deconvoluted, and examined with the Bruker M6 Jetstream software, while the spectra of the more recently analysed purses were treated with Datamuncher in combination with PyMCA. Datamuncher is an open-source tool for fast qualitative XRF imaging data processing [36] that operates in conjunction with PyMCA, which is a collection of open-source Python tools for spectral data analysis with a focus on XRF [37]. Chemical elements were identified by fitting the summed spectrum and maximum pixel spectrum [38]. Due to software incompatibility, it was not possible to also use the Datamuncher and PyMCA software for deconvolution of the spectra of the mitres. For these maps spectra were deconvoluted with the M6 software and specific emission lines were used as mentioned in the results. The results were qualitatively interpreted based on the distribution maps. Each distribution map obtained for a given element in the measured area is a plot in greyscale, where a black colour represents the absence of the element, white represents its abundance, and the intermediate greyscale represents quantities in between.

The multi-layered structure and the undulated surfaces of the mitres (Fig. 4) present complications for the possibilities of MA-XRF mapping. Therefore, analysis locations were restricted to more-or-less flat areas and was thus the determining factor for the size of the scans performed. Depending on the object, the mapping measurements were performed in several smaller zones (maximum area of 58 cm^2) and the working distance

was adjusted for each scan to avoid any contact with the object. The lateral resolution is determined by the beam spot size chosen and the pixel size (i.e. the distance between two measurement points). These parameters and the dwell time (time per pixel) are chosen partly as a function of the size of the area to be scanned, to achieve a balance between resolution and a realistic total measurement time. For the mitres, the scans were taken using a $150 \mu\text{m}$ X-ray beam spot size, $100 \mu\text{m}$ pixel size, and 10 ms per pixel. The overlap created by using an incident beam spot size of $150 \mu\text{m}$ and $100 \mu\text{m}$ distance between two measurement points improves the signal and image resolution. For the analysis of the purses, the scans were made with $150 \mu\text{m}$ beam spot size, a pixel size of $125 \mu\text{m}$, and 20 ms pixel time, which resulted in a total analysis time of $5\text{h}53 \text{ min}$.

The scan of a small surface of the parchment banner on the purse 229f was analysed at higher resolution. Here, the beam spot size was $50 \mu\text{m}$, pixel size was $45 \mu\text{m}$, and scan time was 30 ms per pixel.

Results and discussion

The parchment mitre

MA-XRF mappings were made to identify the composition of a fragment of polychrome parchment positioned centrally on the band on the front side of the parchment mitre. An area of $105.0 \times 54.8 \text{ mm}^2$ with the depiction of two seated apostles was scanned. The results of the MA-XRF mapping for the main elements detected are given as element distribution maps in Fig. 5.

The signal from incident X-rays is typically detectable across all layers from an object due to their high energy, allowing for analysis of materials present from in various pictorial layers. The distribution plot of gold shows its use in the background of the depictions. It is applied as leaf and not as shell gold. The difference in grey value illustrates the 'overlap' of the gold leaf. Heavy elements block X-rays more efficiently than lighter elements, preventing the incident X-rays from reaching underlying layers when there is a high concentration of a heavy element. Hence, a high concentration of gold in one layer may prevent the incident X-ray from reaching underlying layers. This can be seen on the distribution plots of gold, iron, and calcium. In the elemental distribution maps, areas of intense gold signal correlate with areas of less intense calcium and iron, which indicate that both calcium and iron are present under the gold leaf layer. This suggests that the gold was applied over a calcium-containing ground layer (possibly gesso), tentatively coloured by iron oxides, similar as is done for illuminations in manuscripts.

The map with the distribution of lead shows its presence both in the white and in the red coloured areas. This indicates the use of lead white ($2\text{PbCO}_3 \cdot \text{Pb}(\text{OH})_2$)

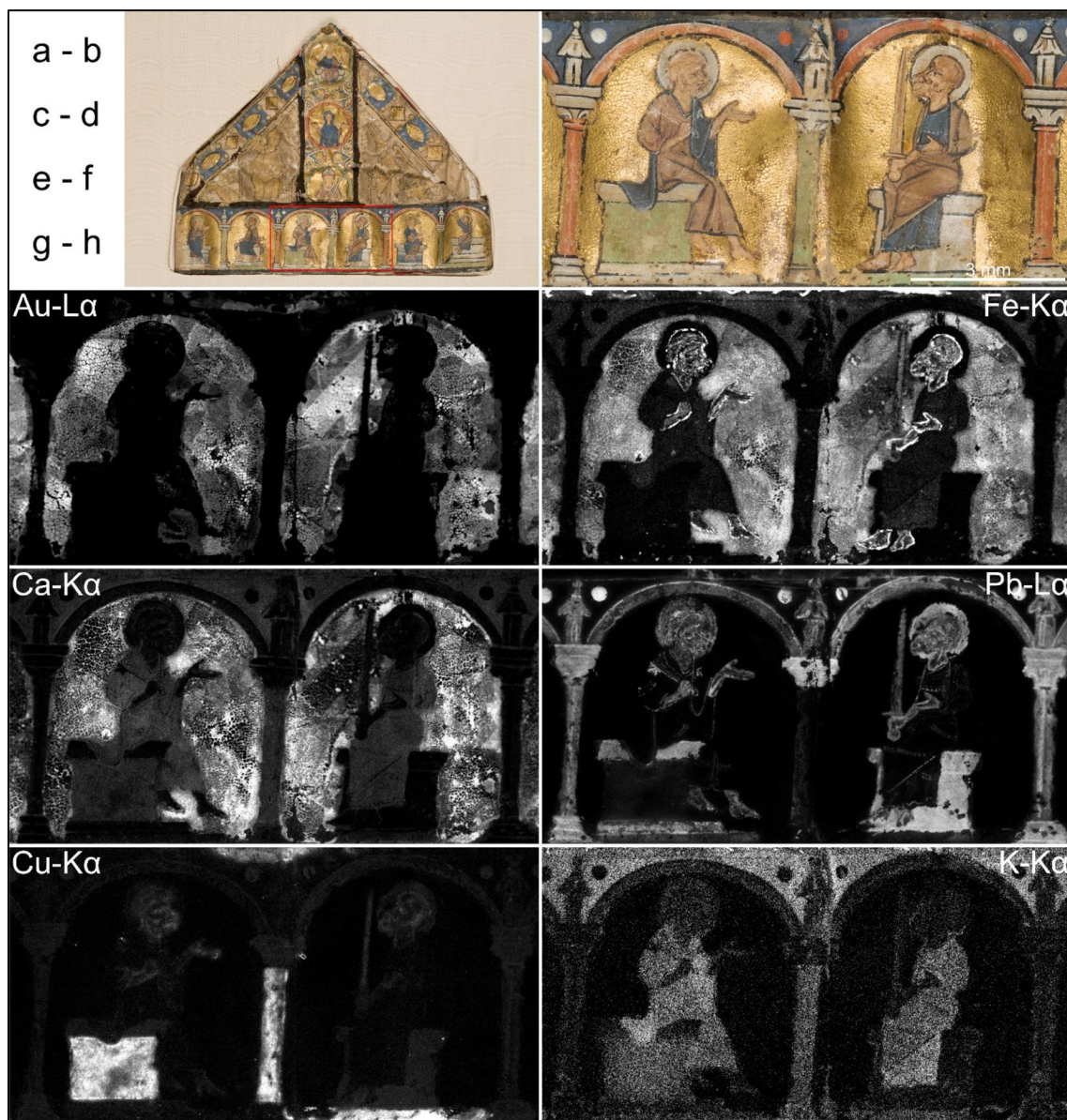


Fig. 5 Depiction of a painted parchment decoration with two seated apostles on the front side of the parchment mitre, with full-size and detail images of the scanned area (a, b) and elemental distribution maps of gold (c), iron (d), calcium (e), lead (f), copper (g), and potassium (h) from a scanned area of $105.0 \times 54.8 \text{ mm}^2$ (reduced image resolution; images©KIK-IRPA, Brussels)

as the white pigment. For the red coloured areas, it suggests the use of red lead (Pb_3O_4), which was confirmed by the molecular characterization of this pigment with micro-Raman measurements (see Additional file 1). Copper is present in the green areas, while the blue areas contain almost no copper. The distribution map of potassium can be interpreted as a possible indication for the use of ultramarine in the blue areas. Although ultramarine $((\text{Na}, \text{Ca})_4(\text{Al}, \text{SiO}_4)_3(\text{SO}_4, \text{S}, \text{Cl}))$ is difficult to map using MA-XRF because of the low atomic

number and the low energy of the constituent elements sodium, silicon, sulfur and aluminum, the presence of potassium in a blue area can indicate a potassium-containing mineral associated with lapis lazuli, originating for over 6000 years from mines in Afghanistan [22, 39–41]. Complementary analysis with micro-Raman spectroscopy allowed the use of ultramarine to be confirmed (see Additional file 1).

A second MA-XRF mapping was performed on a $45.4 \times 70.7 \text{ mm}^2$ area on the front side of the mitre, on an

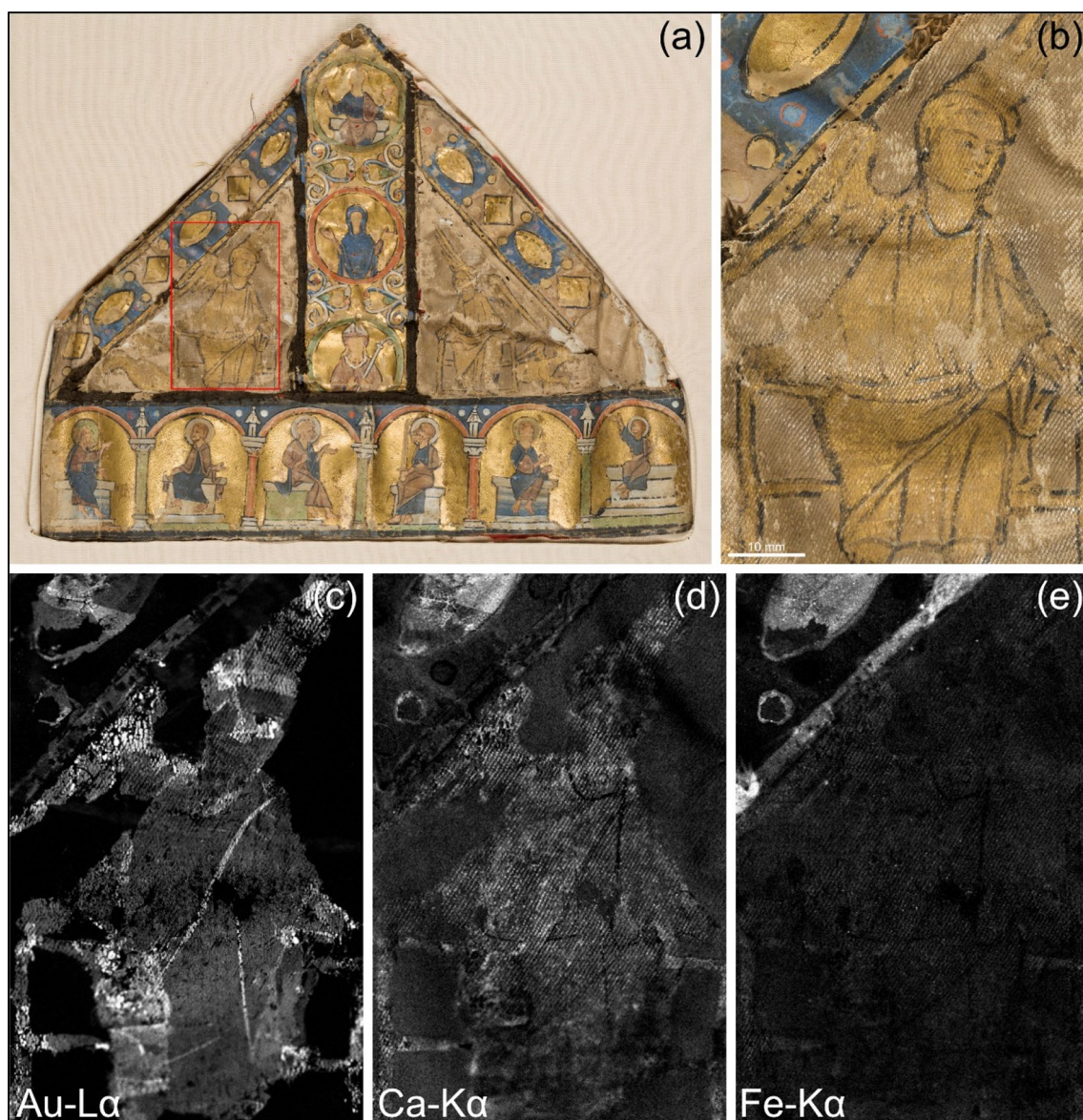


Fig. 6 Depiction of an angel painted on the degraded silk samite on the front side of the mitre with full-size and detail images of the scanned area in red (**a**, **b**) and elemental distribution plots of gold (**c**), calcium (**d**), and iron (**e**) from a scanned area $45.4 \times 70.7 \text{ mm}^2$ (reduced image resolution; images©KIK-IRPA, Brussels)

angel figure painted directly on the silk, which is highly degraded (Fig. 6). The distribution of gold shows that gold leaf was also used in this region. It also indicates certain areas from the figure where gold is more abundant. The gold leaf was applied to a calcium-containing underlayer but did not coincide with iron here. However, iron was detected in the upper left corner of the analysed area, corresponding to a gold-painted oval decoration and gold-painted border of a small parchment band, suggesting the use of a calcium-iron based ground layer, as with the previous scan.

A third area of interest for MA-XRF mapping was an area at the back side of the parchment mitre where adjustments were made by means of a metal thread braided band, tentatively to adjust the circumference of the mitre to the head circumference of the individual for whom it is intended. Since the surface of interest has quite a lot of relief, it was not an ideal location for a mapping. However, it was possible to take a MA-XRF mapping on a squared area of $50.0 \times 49.5 \text{ mm}^2$ (Fig. 7). The iron and gold distribution maps show that the vertical band of polychrome parchment decoration continues

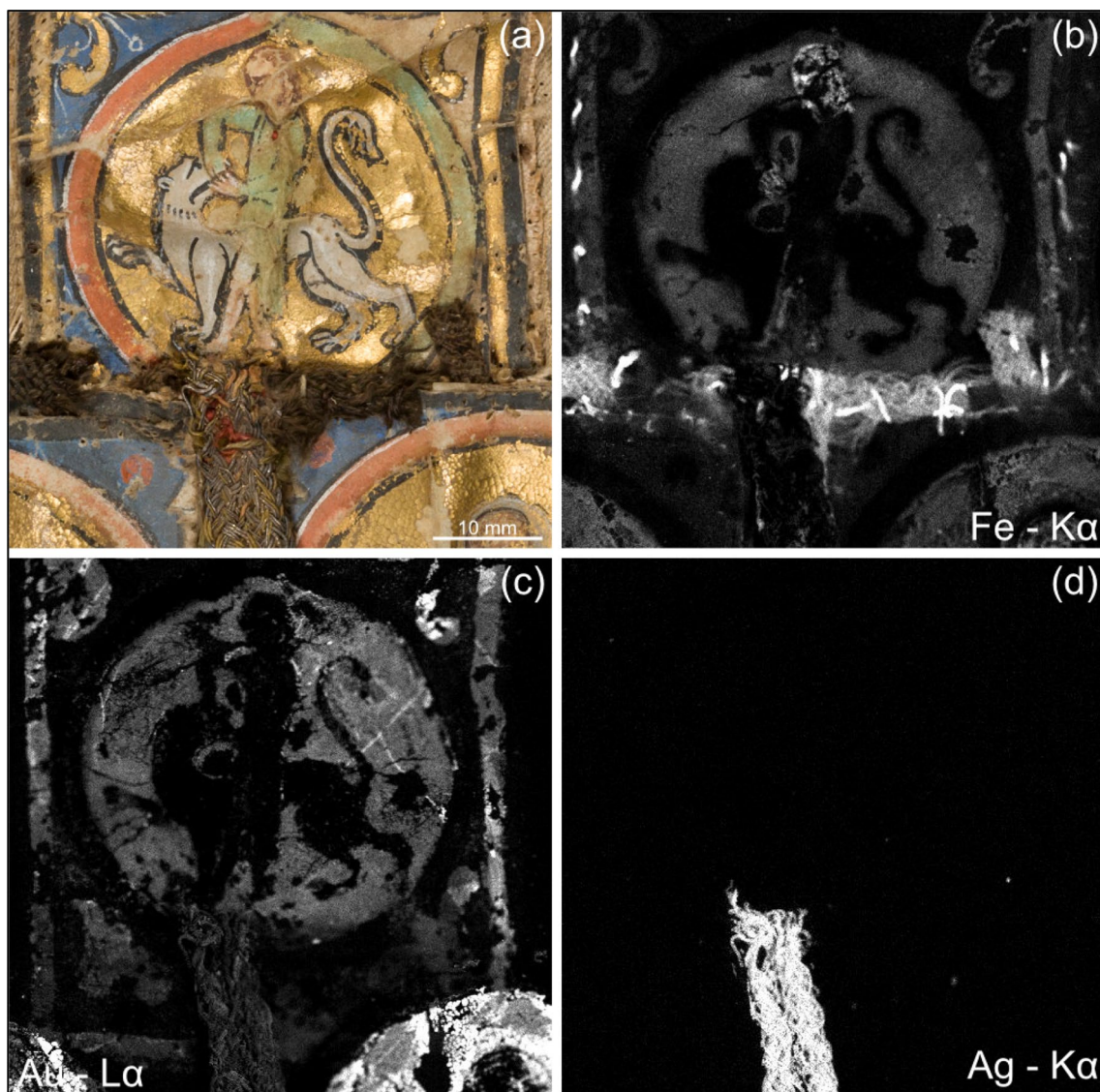


Fig. 7 Scanned area of 50.0 x 49.5 mm² of the construction with the braided band at the back side of the mitre (a) with elemental distribution plots of iron (b), gold (c), and silver (d) (reduced image resolution; images©KIK-IRPA, Brussels)

underneath the horizontal one, hence revealing the way in which the mitre was constructed or adapted at a later stage. The distribution maps also give information about the composition of the metal threads used for the braided band. The distribution maps indicate that the braid consists mainly of metal threads made of silver. In addition, the gold distribution map shows that gilded silver threads were used, the gilding of which may have partially disappeared. Alternatively, the lower intensity of the gold signal is possibly partly due to the overlapping of the metal threads among themselves in the "braid" construction, which may result in a more diffuse signal of the measured induced X-ray fluorescence. The presence of

one-sided gilded silver threads was confirmed by SEM-EDS analysis.

Further MA-XRF mapping of the vertical band with illuminated parchment decorations at the back side of the mitre (43.8 x 95.9 mm²) revealed the presence of several silver threads not visible to the eye, as shown in Fig. 8a–b. Detaching the back and front piece of the mitre revealed the completely hidden interior of the original three-dimensional shape of the mitre head. Inside, there is a very damaged ecru silk samite fabric decorated with painted motifs of stars and moons enriched with silver threads (Fig. 8c). The original three-dimensional shape of the mitre corresponds to the model in use in the

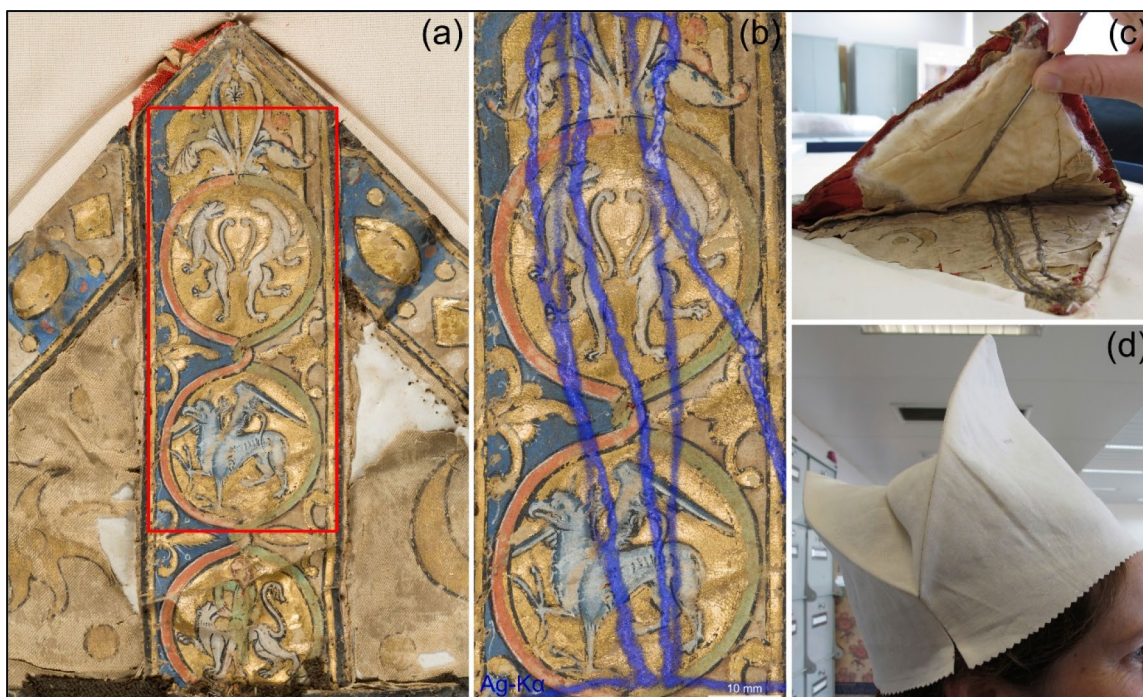


Fig. 8 Measured area of $43.8 \times 95.9 \text{ mm}^2$ of the vertical band at the back side of the mitre with illuminated parchment decoration with selection of the scanned area (a); MA-XRF video image together with the element distribution of silver shown in blue (b); Image of the interior of the mitre head after opening (c) and a 3D-reconstruction of the mitre head (d) (reduced image resolution; images©KIK-IRPA, Brussels)

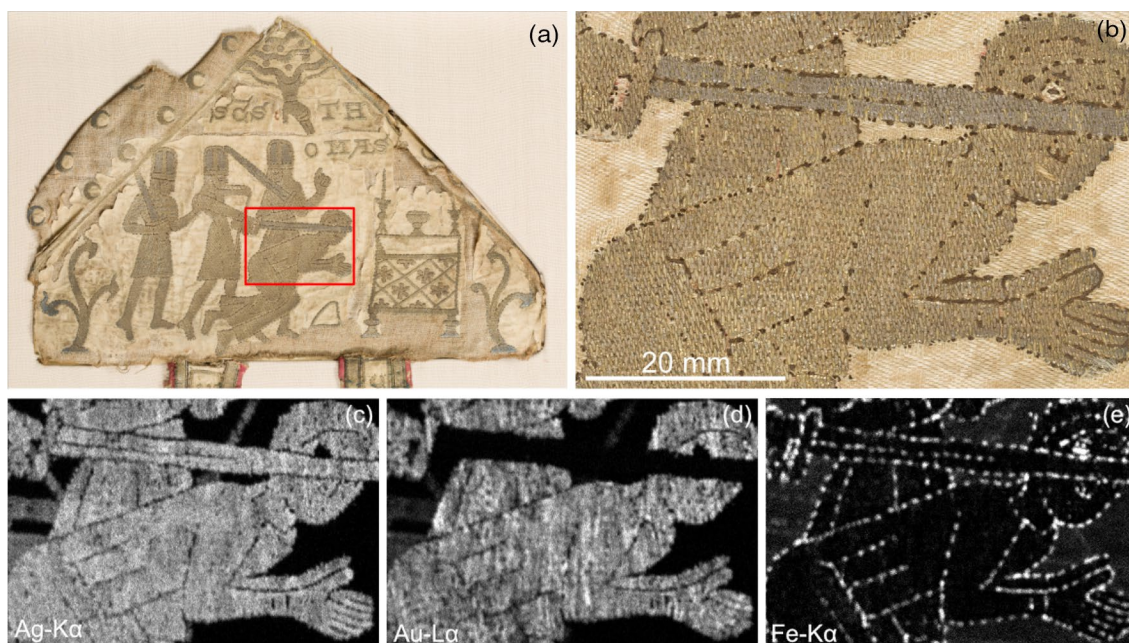


Fig. 9 Depiction of the assassination of Saint Thomas Becket on the reverse side of the embroidery mitre, with full-size and detail images of the mapping area (a, b), and element distribution of silver (Ag) (c), gold (Au) (d), and iron (Fe) (e) from a scanned area of $38.7 \times 57.4 \text{ mm}^2$ (reduced image resolution; images©KIK-IRPA, Brussels)

thirteenth century, with reduced height and fanons. Since the tenth century, mitres have been traditionally associated with popes, cardinals, and bishops and are generally classified according to the decoration. A mitre decorated with precious metals and gemstones is called *mitra pretiosa*. This parchment mitre, for which the precious gems are only suggested by the illumination, can be considered a lighter and less expensive ‘travel’ version of a *mitra pretiosa* [30, 42]. A reconstruction was made by the textile restorers of the original 3-dimensional shape of the mitre head (Fig. 8d).

The embroidered mitre

From the textile mitre, a MA-XRF mapping was made of the metal thread embroidery of the depiction of the assassination of Saint Thomas Becket in the centre of the reverse side of the mitre head. A rectangular area of $38.7 \times 57.4 \text{ mm}^2$ of the central metal thread embroidery was analysed (Fig. 9a, b). The distribution plots for silver and gold (Fig. 9c, d) visualize the use and distribution of silver and gilded silver threads in the scanned decoration. The sword only contains silver while the persons are depicted in the silver and gold distribution plots, indicating for the use of gilded silver threads. The scene presented was made exclusively by embroidery in silver and gilded silver threads.

In addition, iron was also measured. The distribution plot of iron indicates that it completely coincides with

a black thread which was used to frame the figures. The presence of iron can be related to the dyeing of the textile thread. As with black ink for manuscripts [43], iron salts are well-known ingredients in the black dyeing of wool and silk yarns [44]. Dyeing threads black with iron sulphates (vitriol) and tannins was the most common way of obtaining a saturated black colour on silk in the Middle Ages and until the end of the eighteenth century [45, 46]. Micro-destructive analysis with HPLC–DAD of a loose end of a black thread confirmed the use of tannin derived from galls or sumac by the detection of ellagic acid (see Additional file 1). The MA-XRF distribution plot maps where this dyed yarn was used throughout the scanned area. The identification of the iron in the single black contour yarn also demonstrates that MA-XRF could be used to identify other metallic mordants in dyed wool or silk yarns, such as tin- and copper-containing mordants. This was confirmed by testing with reference samples but has not been encountered thus far in heritage textiles.

The Spanish reliquary purse

MA-XRF mapping was performed of the medieval purse of Spanish origin 229d. The front and back of the purse were scanned in entirety, measuring an area of $119 \text{ mm} \times 124 \text{ mm}$. The distribution maps of gold, silver, and copper measured on both sides of the purse are shown in Fig. 10. Scanning one side of the purse identified not only the elemental distribution on that side, but

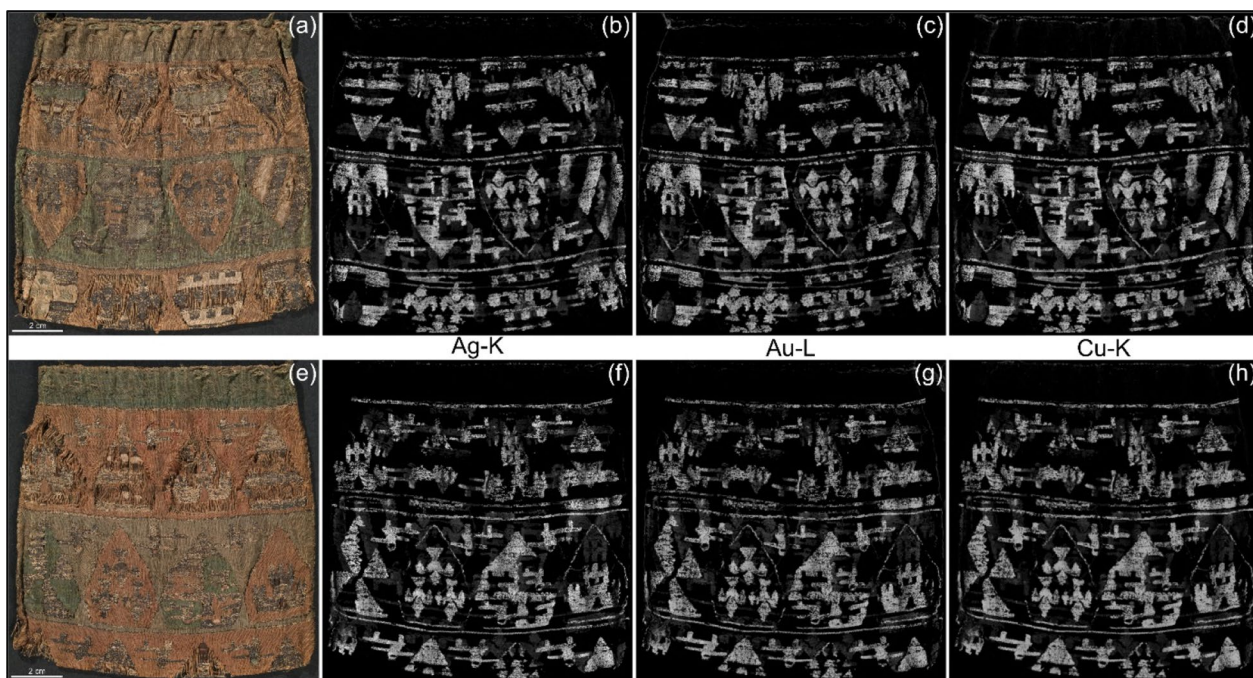


Fig. 10 Image of front (a) and reverse (e) side of the Spanish purse 229d, with elemental distribution plots of silver (b–f), gold (c–g) and copper (d–h) measured for both sides, scanned area of $119.1 \times 123.9 \text{ mm}^2$ (reduced image resolution; images©KIK-IRPA, Brussels)

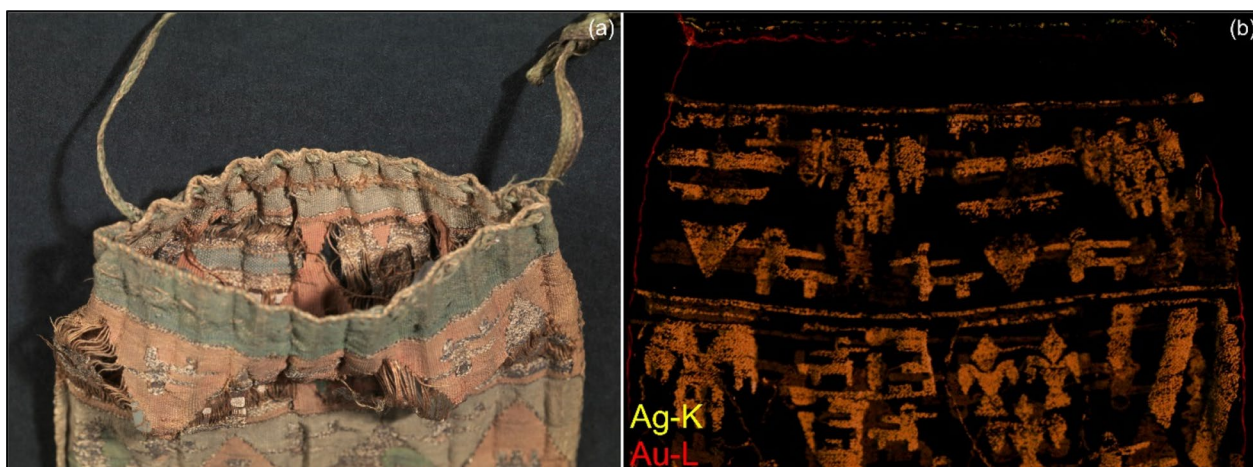


Fig. 11 Detail of the opening at the top of the purse (a) with the superposition of the silver (yellow) and the gold (red) distribution plots showing the golden thread at the top and left side of the purse (b) (reduced image resolution; images©KIK-IRPA, Brussels)

also that of the reverse side, making the scans more difficult to interpret. Ideally, the MA-XRF mapping would be performed by placing a lead plate inside the purse to avoid measuring elements in the underlying textile. However, this was not an option in this case due to the fragility of the object. The distribution maps of gold and silver show that both elements overlap significantly. An additional analysis was performed with SEM-EDS on a sample of a metal thread end taken from a degraded section in the central part of the purse. The analyses from both sides of the lamella indicate that a one-sided gilded

silver lamella was used (see Additional file 1), with a Ag/Cu ratio of 96/4 (weight %). The lamella was wrapped in an s-twist around a core yarn of undyed silk. This type of gilded silver thread was made by using gilded sheets of silver which were hammered into a very thin sheet and then cut into fine strips for making the spun thread. Such metal threads were used all over Europe during the twelfth and thirteenth century mainly for embroidery [47]. Superposition of the gold and silver plots (Fig. 11b) revealed the presence of a fine gold thread at the top edge of the purse, which continues along the left side of the

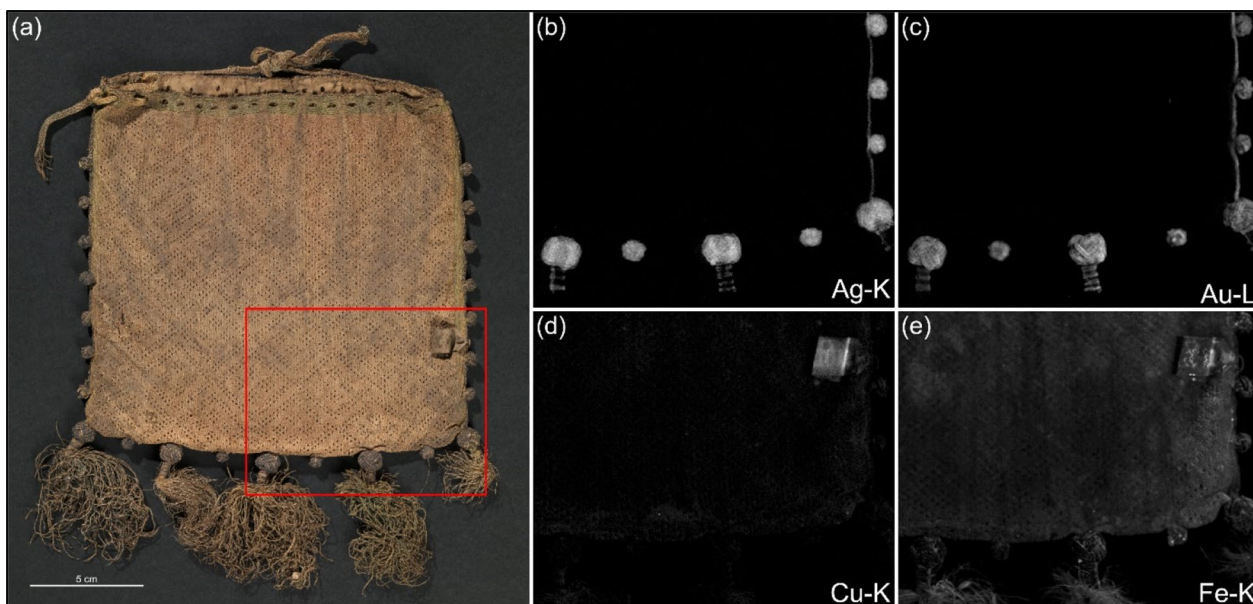


Fig. 12 Image of the front side of the purse in needlework 229f with indication of the area of measurement (a) and elemental distribution plots of silver (b), gold (c), copper (d), and iron (e) from a scanned area of $100.0 \times 81.5 \text{ mm}^2$ (reduced image resolution; images©KIK-IRPA, Brussels)

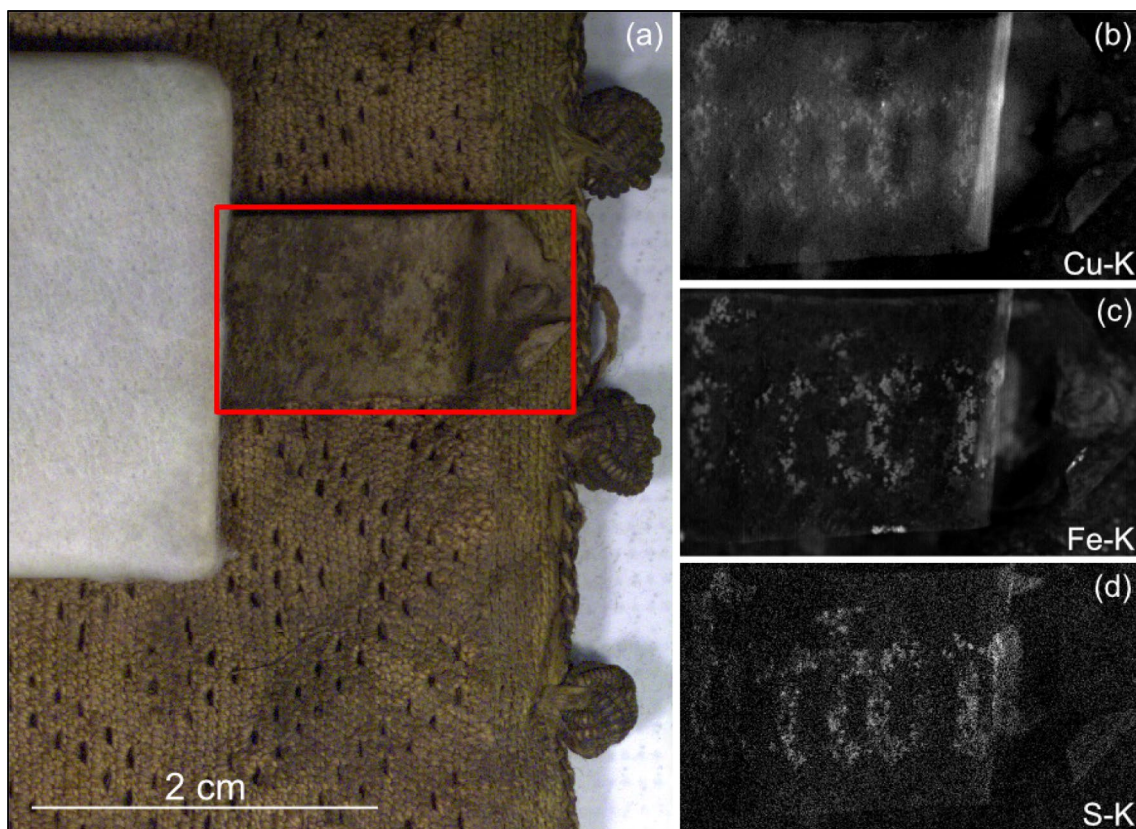


Fig. 13 Small parchment band with indication of the scanned area of $20.4 \times 11.9 \text{ mm}^2$ (a), with MA-XRF distribution plots of copper (b), iron (c), and sulphur (d) (reduced image resolution; images©KIK-IRPA, Brussels)

purse and likely along the right side as well. This thread is not visible on the outside of the purse (Fig. 11a).

The reliquary purse in needlework

MA-XRF mapping was performed on an area of $100.0 \times 81.5 \text{ mm}^2$ of a reliquary purse (229f) including needlework, Turk's head knots, and a very small parchment banner. The distribution plots of gold and silver show that the knots were made with gilded silver threads which are connected to each other, as can be seen at the right side of the purse. Copper and iron were found on the parchment (Fig. 12). Therefore, an additional MA-XRF mapping was made at higher resolution of the entire (outstretched) banner, with a scanned area of $20.4 \times 11.9 \text{ mm}^2$. A lead plate covered with paper was used to stretch the banner during the analysis. The distribution plots of iron, copper, and sulphur reveal the presence of writing (Fig. 13), most likely written with iron gall ink. The vitriol used for the preparation of the ink contains not only iron sulphate but also copper [43]. Unfortunately, the inscription remains illegible.

Conclusion

MA-XRF mapping analyses were successfully applied for the non-invasive examination of the Episcopal mitres and the medieval reliquary purses from Namur. The technique proved to be very useful for identification of inorganic elements, although complementary analytical techniques were sometimes needed to confirm the elemental observations. MA-XRF identified elements of materials used in painted and embroidered textiles and in parchment illuminations, such as the gilded silver and silver threads, iron-based dyes and inks, gold leaf, lead and copper pigments, and calcium- and/or iron-containing underlayers.

In addition to material identification, the MA-XRF maps provided a clear visualization of the distribution of each element over the scanned area, making it possible to identify which elements coincide and where. This was very useful for obtaining stratigraphic information in multi-layered structures, such as the use of gold leaf on a calcium and iron-containing underlayer, or to reveal the presence of elements associated with materials not

visible on the surface. In this way, hidden materials were detected, and manufacturing details revealed.

While MA-XRF is well-established for the analysis of objects with a flat surface, it is less straightforward in the case of multi-layered textile objects or textiles with relief. This was the case with the mitres, for which MA-XRF analyses were limited by the undulated surface. The problem was partially resolved by performing measurements on smaller areas and adjusting the working distance for each scan separately to the upper part of the measurement area to avoid any contact with the surrounding areas. However, this also meant that only lower resolutions could be obtained for those sections.

Finally, in situations where it is very difficult to sample or where a sample cannot be taken accurately based on visual selection, instrumental techniques that make material or structural details visible across a larger area add significant value. In addition to material identification, MA-XRF element distribution maps of the mitres and purses also helped to ensure that sampling was carried out at a more informative and representative location, thus minimizing sampling.

Abbreviations

MA-XRF	Macro-X-ray fluorescence
SEM-EDS	Scanning electron microscopy with energy dispersive X-ray spectroscopy
(HP)LC	(High performance) liquid chromatography
DAD	Diode array detection
GC	Gas chromatography
MRS	Micro-Raman spectroscopy
(ATR)-FTIR	(Attenuated total reflectance) Fourier transform infrared spectroscopy

Supplementary Information

The online version contains supplementary material available at <https://doi.org/10.1186/s40494-023-00977-6>.

Additional file 1: Figure 1: Raman spectra of a red (a) and a blue (b) area (in red) of the painted apostle depiction of the parchment mitre, together with the reference spectra of red lead (a) and ultramarine (b) (in blue).

Figure 2: Dye identification of a black contour yarn from the mitres. HPLC-DAD chromatogram (255 nm) and absorbance spectrum of ellagic acid.

Figure 3: Microscope image of the metal strip of a sampled metal thread end from the Spanish reliquary purse 229d (a); Backscattered electron image of the lamella with indication of the areas of analyses (b) and element spectra (sp40) at the inner (c) and (sp41) at the outer side (d) of the lamella (images©KIK-IRPA, Brussels).

Acknowledgements

We are very thankful to Brynn Sundberg for the language correction.

Author contributions

IVB: conceptualization, methodology, analysis, data interpretation and image treatment, writing original draft, major contributor of the manuscript. MVB: methodology, analysis, data interpretation and image treatment, reporting, writing original draft. MV: analysis, data interpretation and image treatment, reporting. AC: data interpretation and image treatment. All authors read and approved the final manuscript.

Funding

This publication is based on work by/and funded by the COST Action "Europe Through Textiles: Network for an integrated and interdisciplinary Humanities" - EuroWeb, CA19131, supported by COST (European Cooperation in Science and Technology). COST is a funding agency for research and innovation networks. Our Actions help connect research initiatives across Europe and enable scientists to grow their ideas by sharing them with their peers. This boosts their research, career and innovation. www.cost.eu. The MA-XRF mapping of Bishop de Vitry's mitres was performed in addition to the material-technical study carried out within the framework of the interdisciplinary scientific research project *Études croisées en Histoire et en Sciences exactes sur les mitres et les ossements de l'évêque Jacques de Vitry* (CROMIOSS), a project launched in 2015 by The Archaeological Society of Namur with the financial support of the King Baudouin Foundation.

Availability of data and materials

The data that support the findings of this study are available from the corresponding author on reasonable request and with the permissions of The Archaeological Society of Namur and the King Baudouin Foundation.

Declarations

Competing interests

The authors declare that they have no competing interests that could influence the work reported in the manuscript.

Received: 1 February 2023 Accepted: 17 June 2023

Published online: 30 August 2023

References

- Degano I, Biesaga M, Colombini MP, Trojanowicz M. Historical and archaeological textiles: an insight on degradation products of wool and silk yarns. *J Chromatogr A*. 2011;1218(34):5837–47.
- Vanden Berghe I. Towards an early warning system for oxidative degradation of protein fibres in historical tapestries by means of calibrated amino acid analysis. *J Archaeol Sci*. 2012;39(5):1349–59. <https://doi.org/10.1016/j.jas.2011.12.033>
- Margariti C. The application of FTIR microspectroscopy in a non-invasive and non-destructive way to the study and conservation of mineralised excavated textiles. *Herit Sci*. 2019. <https://doi.org/10.1186/s40494-019-0304-8>.
- Davis M, Harris S. Textiles in a Viking Age hoard: Identifying ephemeral traces of textiles in metal corrosion products. *J Archaeol Sci Rep*. 2023. <https://doi.org/10.1016/j.jasrep.2022.103796>.
- Skals I, Gleba M, Taube M, Mannering U. Wool textiles and archaeometry: testing reliability of archaeological wool fibre diameter measurements. *Danish J Archaeol*. 2018;7(2):161–79.
- Vanden Berghe I, Gleba M, Mannering U. Towards the identification of dyestuffs in early iron age scandinavian peat bog textiles. *J Archaeol Sci*. 2009;36(9):1910–21. <https://doi.org/10.1016/j.jas.2009.04.019>
- Tamburini D, Dyer J, Vandenbeusch M, Borla M, Angelici D, Aceto M, et al. A multi-scalar investigation of the colouring materials used in textile wrappings of Egyptian votive animal mummies. *Herit Sci*. 2021. <https://doi.org/10.1186/s40494-021-00585-2>.
- Karatzani A. The use of metal threads in the decoration of late and post-byzantine embroidered church textiles. *Cahiers Balkaniques*. 2021;17:48.
- Petrovicu I, Vanden Berghe I, Cretu I, Albu F, Medvedovici A. Identification of natural dyes in historical textiles from Romanian collections by LC-DAD and LC-MS (single stage and tandem MS). *J Cult Herit*. 2012;13(1):89–97.
- Gleba M, Bretones-García MD, Cimarelli C, Vera-Rodríguez JC, Martínez-Sánchez RM. Multidisciplinary investigation reveals the earliest textiles and cinnabar-coloured cloth in Iberian Peninsula. *Sci Rep*. 2021. <https://doi.org/10.1038/s41598-021-01349-5>.
- Wetz J, Quye A, France D, Tang PL, Richmond L. Authenticating Turkey red textiles through material investigations by FTIR and UHPLC. In: ICOM-CC

- 18th Triennial Conference Preprints, Copenhagen. Bridgland J. Paris: International Council of Museums; 2017;1–8.
12. Janssens K, Vittiglio G, Deraedt I, Aerts A, Vekemans B, Vincze L, et al. Use of microscopic XRF for non-destructive analysis in art and archaeometry. *X-Ray Spectrom.* 2000;29(1):73–91.
13. Shugar AN, Mass JL, Smith D. *Handheld XRF for art and archaeology.* Leuven, Belgium: Leuven University Press; 2012.
14. Clarke M. The analysis of medieval European manuscripts. *Stud Conserv.* 2001;46(sup1):3–17.
15. Klišińska-Kopacz A. Nondestructive testing of historic textiles. In: Seiko J, Sabu T, Pintu P, Ritu P, editors. *Handbook of museum textiles.* Hoboken: Wiley Online Library; 2022.
16. Alfeld M, Pedroso JV, van Eikema HM, Van der Snickt G, Tauber G, Blaas J, et al. A mobile instrument for in situ scanning macro-XRF investigation of historical paintings. *J Anal At Spectrom.* 2013;28(5):760.
17. Van der Snickt G, Martins A, Delaney J, Janssens K, Zeibel J, Duffy M, et al. Exploring a hidden painting below the surface of René Magritte's le portrait. *Appl Spectrosc.* 2016;70(1):57–67.
18. Van der Snickt G, Dubois H, Sanyova J, Legrand S, Coudray A, Glaude C, et al. Large-area elemental imaging reveals van Eyck's original paint layers on the Ghent Altarpiece (1432). *Rescoping Its Conser Treatment Angewandte Chemie.* 2017;129(17):4875–9.
19. Alfeld M, Siddons DP, Janssens K, Dik J, Woll A, Kirkham R, et al. Visualizing the 17th century underpainting in portrait of an old man by Rembrandt van Rijn using synchrotron-based scanning macro-XRF. *Appl Phys A.* 2012;111(1):157–64.
20. Alberti R, Frizzi T, Bombelli L, Gironda M, Aresi N, Rosi F, et al. CRONO: a fast and reconfigurable macro X-ray fluorescence scanner for in-situ investigations of polychrome surfaces. *X-Ray Spectrom.* 2017;46(5):297–302.
21. Romano FP, Caliri C, Nicotra P, Di Martino S, Pappalardo L, Rizzo F, et al. Real-time elemental imaging of large dimension paintings with a novel mobile macro X-ray fluorescence (MA-XRF) scanning technique. *J Anal At Spectrom.* 2017;32(4):773–81.
22. Ricciardi P, Legrand S, Bertolotti G, Janssens K. Macro X-ray fluorescence (MA-XRF) scanning of illuminated manuscript fragments: potentialities and challenges. *Microchem J.* 2016;124:785–91.
23. Watteeuw L, Van Bos M, Gersten T, Vandermeulen B, Hameeuw H. An applied complementary use of macro X-ray fluorescence scanning and multi-light reflectance imaging to study medieval illuminated manuscripts. *The rijmbijbel of Jacob van Maerlant.* Microchem J. 2020. <https://doi.org/10.1016/j.microc.2019.104582>.
24. Van der Snickt G, Legrand S, Caen J, Vanmeert F, Alfeld M, Janssens K. Chemical imaging of stained-glass windows by means of macro X-ray fluorescence (MA-XRF) scanning. *Microchem J.* 2016;124:615–22.
25. Mabrouk N, Elsayed Y. Archaeometrical study of a rare embroidered and appliqued leather tapestry from the Safavid artworks part II: colored leather. *Mediterr Archaeol Archaeometry.* 2020;20(3):1–12.
26. Saverwyns S, Currie C, Lamas-Delgado E. Macro X-ray fluorescence scanning (MA-XRF) as tool in the authentication of paintings. *Microchem J.* 2018;137:139–47.
27. Vermeulen M, Tamburini D, McGeachy AC, Meyers RD, Walton MS. Multiscale characterization of shellfish purple and other organic colorants in 20th-century traditional enredos from Oaxaca. *Mexico Dyes Pigments.* 2022;206: 110663.
28. Mosca S, Frizzi T, Pontone M, Alberti R, Bombelli L, Capogrosso V, et al. Identification of pigments in different layers of illuminated manuscripts by X-ray fluorescence mapping and Raman spectroscopy. *Microchem J.* 2016;124:775–84.
29. Galli A, Caccia M, Alberti R, Bonizzoni L, Aresi N, Frizzi T, et al. Discovering the material palette of the artist: a p-XRF stratigraphic study of the Giotto panel "God the Father with Angels." *X-Ray Spectrom.* 2017;46(5):435–41.
30. Lebecque F. Final Report Project CROMIOSS: Études Croisées en Histoire et en Sciences exactes sur les Mitres et les Ossements de l'Évêque Jacques de Vitry; 2018 (unpublished) 47 p.
31. Donnadieu J. Jacques de Vitry (1175/1180–1240). *Entre l'Orient et l'Occident: l'évêque aux trois visages.* Turnhout: Brepols Publishers; 2015.
32. Decorte R, Polet C, Boudin M, Tilquin F, Matroule J-Y, Dieu M, et al. An interdisciplinary study around the reliquary of the late cardinal Jacques de Vitry. *PLoS ONE.* 2019;14(2):e0201424.
33. Sorber F. *Technological Study of the Mitres of Jacques de Vitry;* 2018 (unpublished) 6 p.
34. Robinet C. *Les peintures à l'aiguille.* In: *Guide du visiteur no.9.* Namur: Musée Provincial des Arts Anciens Namurois; 2007. Namur, Imprimerie provinciale
35. Damen E, Kockelkoren, G, Goris J, Vanden Berghe I, Van Bos M, Boudin M. KIK-IRPA Final Report material-technical study and conservation, preservation, and presentation treatment of seven reliquary purses of the Archaeological Society in Namur (SAN); 2021 (unpublished) 109 p.
36. Alfeld M, Janssens K. Strategies for processing mega-pixel X-ray fluorescence hyperspectral data: a case study on a version of Caravaggio's painting Supper at Emmaus. *J Anal At Spectrom.* 2015;30(3):777–89.
37. Solé VA, Papillon E, Cotte M, Walter Ph, Susini J. A multiplatform code for the analysis of energy-dispersive X-ray fluorescence spectra. *Spectrochim Acta Part B Atomic Spect.* 2007;62(1):63–8.
38. Bright DS, Newbury DE. Maximum pixel spectrum: a new tool for detecting and recovering rare, unanticipated features from spectrum image data cubes. *J Microsc.* 2004;216(2):186–93.
39. Watteeuw L, van Bos M. A manuscript for the head: The study and conservation of the thirteenth-century illuminated parchment mitre of Bischof Jacques de Vitry. In: *Care and conservation of manuscripts.* Museum Tusulanum Press; 2023. p. 417–34.
40. Plester J. Chapter 2: Ultramarine Blue, Natural and Artificial. In: *Artists' Pigments, a Handbook of their History and Characteristics. Volume 2.* Washington: National Gallery of Art; London: Archetype publications; 1993; 37–56.
41. Eastaugh N, Walsh V, Chaplin T, Siddall R. *Pigment compendium. A dictionary of historical pigments.* Oxford: Elsevier Butterworth-Heinemann publication; 2008.
42. Nainfa JA. *Costume of prelates of the catholic church according to roman etiquette new and revised.* Baltimore: John Murphy Company; 1926. p. 145–7.
43. Watteeuw L, van Bos M. Composition of iron gall inks in illuminated Manuscripts (11th–16th century). *The Use by Scribes and Illuminators.* In: *Care and Conservation of Manuscripts.* Copenhagen: The Arnamagnæan Institute, University of Copenhagen, Museum Tusulanum Press; 2014;365–81 p.:18–36.
44. Ortega Saez N, Vanden Berghe I, Schalm O, De Munck B, Caen J. Material analysis versus historical dye recipes: ingredients found in black dyed wool from five Belgian archives (1650–1850). *Conserv Património.* 2019;10(31):115–32.
45. Brunello F. *The art of dyeing in the history of mankind.* Vicenza: Neri Pozza; 1973.
46. Takami M, Vanden Berghe I. Caring for the queen Victoria's privy council dress c. 1837: an investigation of the unique discoloration of the black silk. *e-Preservation Sci.* 2013;10:42–9.
47. Karatzani A. Metal threads: the historical development. In: *Proceedings of the Traditional Textile Craft: An Intangible Cultural Heritage.* 2012. p. 163–74.

Publisher's Note

Springer Nature remains neutral with regard to jurisdictional claims in published maps and institutional affiliations.

Ina Vanden Berghe IVB Head of the Textile Research Lab of the Laboratory Department of the KIK-IRPA and senior scientist in the Lab of Paper, Leather & Parchment. She specialised in the fields of material technical and degradation studies of textiles, leather, and parchment (natural and synthetic organic dyes, metals, mordants, proteins) with various techniques.

Marina Van Bos MVB Head of the Lab of Paper, Leather & Parchment at the KIK-IRPA and senior scientist in the Lab of Monuments

and Monumental Decoration with a long experience in the material and degradation analyses of illuminated manuscripts and mural paintings with various techniques.

Maike Vanderpe MV technical assistant carrying out analyses for the Research Labs of Textiles, Paper, Leather & Parchment and Monuments & Monumental decorations at the KIK-IRPA.

Alexia Coudray AC scientist carrying out analyses for the Research Labs of Textiles and Paintings at the KIK-IRPA.

Submit your manuscript to a SpringerOpen[®] journal and benefit from:

- ▶ Convenient online submission
- ▶ Rigorous peer review
- ▶ Open access: articles freely available online
- ▶ High visibility within the field
- ▶ Retaining the copyright to your article

Submit your next manuscript at ▶ [springeropen.com](https://www.springeropen.com)
